Self-trapping of vortex crystals via competing nonlinearities

Angel Paredes and Humberto Michinel
Instituto de Física e Ciencias Aeroespaciais (IFCAE), Universidade de Vigo. Campus de As Lagoas, E-32004 Ourense, Spain

(Received 14 November 2023; accepted 18 January 2024; published 22 February 2024)

We investigate the existence of self-trapped nonlinear waves with multiple phase singularities. Working with the cubic-quintic nonlinear Schrödinger equation, we focus on configurations with an antivortex surrounded by a triangular arrangement of vortices within a hosting soliton. We find stationary patterns that can be interpreted as stable self-trapped vortex crystals, constituting the first example of a configuration of this sort with space-independent potentials. Their stability is linked to their norm, transitioning from unstable to stable as their size increases, with an intermediate region where the structure is marginally unstable, undergoing a remarkable and puzzling self-reconstruction during its evolution.

DOI: 10.1103/PhysRevE.109.024216

I. INTRODUCTION

Localized self-trapped modes emerge in diverse physical situations as a result of the balance between nonlinearity, diffraction and/or dispersion, with implications for many areas of physics, mathematics and other disciplines [1]. They are usually named solitons abusing language from the original meaning of the term [2], where an integrable one-dimensional problem was considered. Multidimensional [two-dimensional (2D) and three-dimensional (3D)] solitons pave the way to the observation of a variety of interesting phenomena and constitute a broad research topic for both theory and experiment [3–5]. In particular, they allow for the existence of phase dislocations [6], namely vortices, that evolve without distortion and exist in media with repulsive self-interactions [7], for instance in nonlinear optics [8,9] or Bose-Einstein condensates [10,11]. Different versions of the nonlinear Schrödinger equation (NLSE) are useful to model diverse physical situations.

Vortices located at the center of self-trapped beams are usually called bright vortex solitons [12,13]. In this contribution, we disclose the existence of two-dimensional bright solitons pinched by several phase singularities, which we may call multivortex solitons, In particular, we focus on the stationary case, where stationary refers to solutions of the wave equation for which the intensity profile $|\Psi|^2$ remains propagation-invariant. However, it should be noted that some cases are unstable, leading to the eventual unraveling of the initial configuration. These solitons are constructed by arranging the vortex singularities in such a way that their interactions with each other leave the profile invariant. The solutions carry fractional angular momentum, in the sense of Refs. [14–16].

Multivortex solitons have been discussed in the discrete case [17] or in the presence of lattice potentials [18,19]. Arrangements of vortices rotating around a central point have been discussed for nonlocal interactions, giving rise to spiraling multivortex solitons [20]. In a recent interesting paper [21], stationary arrangements of vortices supported by space-dependent nonlinearities were found. Vortex lattices or clusters in Bose-Einstein condensates in rotating traps have been discussed at length, e.g., Ref. [22]. Similar configurations have been found to spontaneously arise in particular laser cavities with dissipation and gain [23]. Our work differs from these cases since we have a self-trapped propagation-invariant profile supported by a space-independent local nonlinear potential.

This novel class of multivortex solitons can be regarded as a self-trapped version of vortex crystals, namely vortex patterns that evolve without change of shape or size [24,25], the simplest example being that of regular polygons [26]. Vortex crystals have been discussed in different physical situations where quantized vortices exist. For instance, Ref. [27] studied regular polygons in Bose-Einstein condensates and Ref. [28] investigated more complicated configurations in superfluids.

Vortex soliton solutions are unstable in many cases, and one of the possibilities for stabilization [29] is the presence of competing nonlinearities [13,30]. In this vein, we work with the cubic-quintic NLSE (CQNLSE), a model with many interesting properties, including the existence of stable bright vortex solitons of arbitrarily high topological charge [31–33]. In optics, that dependence of the refractive index can be achieved for carbon disulfide [34], with solutions of nanoparticles [35] or by appropriately preparing a quantum state within a cold atomic gas, as initially proposed in Ref. [36] and subsequently validated experimentally [37]. The CQNLSE has also been applied to Bose-Einstein condensates, see e.g., Refs. [38,39], superfluids [40] and other fields.

II. SETUP AND FORMALISM

By rescaling, the 2D CQNLSE can be written in the following adimensional form:

$$i\frac{\partial\Psi}{\partial t} = -\nabla^2\Psi + (|\Psi|^4 - |\Psi|^2)\Psi, \tag{1}$$

where $\nabla^2 = \partial_x^2 + \partial_y^2$. Conserved quantities include the norm and angular momentum:

$$N = \int |\Psi|^2 dxdy, \tag{2}$$

$$J = \int \mathrm{Im}[\Psi^*(x\partial_y - y\partial_x)\Psi]dxdy. \tag{3}$$

It is well known that Eq. (1) has flat-top self-trapped solutions with liquidlike properties for large N [41,42]. Using r, θ as polar coordinates in the $x-y$ plane, the vorticity-less solitons are given by $\Psi_{\mathrm{sol}} = e^{i\beta t}\psi_{\mathrm{sol}}(r)$ with $\beta < \beta_{\mathrm{cri}} = \frac{3}{16}$ [43], where the $\psi_{\mathrm{sol}}(r)$ profile can be found numerically by standard methods. When β approaches β_{cr}, the following expression becomes a useful approximation:

$$\psi_{\mathrm{sol}}(r) \approx \frac{\sqrt{3}/2}{\sqrt{e^{\frac{\sqrt{3}}{2}(r-R_{\mathrm{sol}})} + 1}}, \tag{4}$$

where R_{sol} is the soliton radius. We have $R_{\mathrm{sol}} \to \infty$ as $\beta \to \beta_{cr}$. Notice that Eq. (4) represents a flat-top droplet with

$$\psi \approx \psi_{cr} = \sqrt{3}/2 \tag{5}$$

for $r < R_{\mathrm{sol}}$ and $\psi \approx 0$ for $r > R_{\mathrm{sol}}$. There are also dark soliton solutions with vorticity of the form $\Psi = e^{i\beta t}e^{il\theta}\psi_{|l|}(r)$. In the present paper, we will deal with the $|l| = 1$ case, for which we can use a Padé approximant, along the lines of [44]:

$$\psi_{|l|=1} \approx \sqrt{\frac{r^2(606 + 260r^2 + 0.356r^4)}{10^5 - 390r^2 + 360r^4 + 0.475r^6}}. \tag{6}$$

III. MULTIVORTEX POLYGONAL CONFIGURATIONS

We can construct multivortex configurations within a flat-top soliton using Eqs. (4) and (6) as building blocks. Take

$$\psi(x,y) = \frac{\psi_{\mathrm{sol}}(r)}{\psi_{cr}^{n_V}} \prod_{j=1}^{n_V} \psi_{|l_j|}(r_j)e^{il_j\theta_j}, \tag{7}$$

where n_V is the total number of phase dislocations, ψ_{cr} is defined in Eq. (5) and $r_j = \sqrt{(x-x_j)^2 + (y-y_j)^2}$, $\theta_j = \arctan((y-y_j)/(x-x_j))$ are sets of polar coordinates centered at each of the vortices (or antivortices). A particularly interesting case corresponds to placing n vortices of equal l at the vertices of a regular polygon, concentric with the background soliton, i.e.,

$$(x_a, y_a) = R\left(\cos\left(\frac{2\pi a}{n}\right), \sin\left(\frac{2\pi a}{n}\right)\right) \tag{8}$$

with $a = 0, \ldots, n-1$. Note that in our notation, n and n_V can be different integers, as there may be additional singularities beyond those associated with the polygon, as discussed below. These configurations preserve a Z_n rotational symmetry and can rotate rigidly (see Ref. [45] for related studies within a trap).

Flows rotating around the vortex singularities drag other vortices located in their vicinity [8]. The *drag velocity* is perpendicular to the line joining the two vortices and, with the present conventions, its modulus is $2l/\rho$, where l is the topological charge of the vortex inducing the flow and ρ the intervortex distance, see, *e.g.*, Ref. [45]. Let us apply these considerations to a regular n-polygon with l-charged vortices placed at their vertices. The total drag velocity induced in one vortex by the rest of them will be tangential to the circumcircle with modulus:

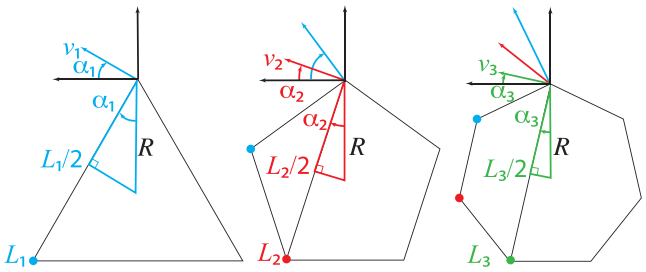

FIG. 1. Schematic vector representation of the dragging velocities induced on the top vortex by others located at the consecutive vertices for various regular polygons. We can see that $\sum_i^{(n-1)} v_{i,\perp} = 4l\sum_i^{(n-1)/2} \frac{\cos(\alpha_i)}{L_i}$ where $R\cos(\alpha_i) = L_i/2$, with L_i the distance between the top vertex to each other vertex, and therefore we immediately derive Eq. (9). This construction, valid for odd n can be easily generalized to even n and the result (9) holds for any integer $n \geqslant 2$.

$$v = \sum_i^{(n-1)} v_{i,\perp} = \frac{l(n-1)}{R}, \tag{9}$$

where $v_{i,\perp}$ is the component of v_i tangential to the circle. Figure 1 provides a graphical illustration of these result. This kind of configuration gives rise to self-trapped spiraling multivortex solutions similar to [20], see the Supplemental Material for an illustrative example [46] of the evolution of a triangle of vortices.

We perform numerical integration of Eq. (1) using the beam propagation method [47] adapting the open source code provided in Ref. [48]. We have controlled the accuracy of the computed evolution by monitoring the conserved quantities. Apart from using small enough spacing for the discretization along x, y, and t, we have found it necessary to use 64-bit floating-point numbers to keep track of the evolution for long simulations as those reported below when discussing the stability.

IV. STATIONARY MULTIVORTEX SOLUTIONS

The main question that we address here is whether stationary solutions $\Psi = e^{i\beta t}\psi(x,y)$ can be constructed by inserting multiple vortex singularities inside a large bright soliton. Namely, we look for self-trapped solutions of the equation:

$$-\beta\psi = -\nabla^2\psi + (|\psi|^4 - |\psi|^2)\psi \tag{10}$$

that have more than one phase dislocation. The simplest generalization of the polygonal configurations of Fig. 1 is to add another vortex, with topological charge l_C, at the center of the droplet. Then, Eq. (9) becomes $v = (2l_C + l(n-1))/R$ and the configuration should remain static if

$$l_C = -l(n-1)/2. \tag{11}$$

In the following, we concentrate on the $l = 1$, $l_C = -1$, $n = 3$ case, namely a singly charged antivortex surrounded by

an equilateral triangle of singly charged vortices [49]. This configuration corresponds to the simplest static vortex crystal [24,25].

Even if the leading contribution to the velocity vanishes, as described above, we find that the triangle rotates, albeit extremely slowly as compared to the case without central antivortex. This happens because there are two subleading contributions that become relevant. One is related to the finiteness of the bright soliton, that can be modeled by introducing image vortices [50]. The second one is related to the nonzero size of the vortex cores. These contributions were discussed in detail in Ref. [45] for a case with external trapping and work in a qualitatively similar fashion in the self-trapped case: for large enough R, the triangle rotates counterclockwise whereas for small enough R it rotates clockwise. By continuity, there must exist a radius R_{st} for which the triangle remains static and, consequently, there is a solution of Eq. (10).

Clearly, Eq. (7) does not provide an exact solution of Eq. (10), but it does provide a good approximation if R is chosen close to R_{st}. Thus, to find our best numerical approximation to stationary solutions we use the following process. First, we choose a hosting bright soliton of a given size and power, therefore fixing $\psi_{\rm sol}(r)$. Then, we run Eq. (1) with initial conditions (7) for different values of the triangle radius R. The result of these simulations show clockwise or counterclockwise rotation of the triangle for different values R and we can find a value R_{st} for which there is no rotation at all. Starting with that initial condition, we use a method of propagation in imaginary time to approach the actual solution [51,52]. Still, this may not fully converge to a completely static configuration but we can further refine the value of R_{st} by running in real time the results of propagation in imaginary time and, again, looking for nonrotating configurations. With this procedure, we find a one-parameter family of solutions, with R_{st} determined as a function of $R_{\rm sol}$ (or, equivalently, of the norm N). Obviously, there is a second, trivial, parameter that can be chosen at will, corresponding to $U(1)$ rotations of the configuration, namely different orientations of the triangle. In Fig. 2, we depict one case and how some of the physical quantities vary along the family.

It is interesting to notice that the stationary solutions have fractional angular momentum, using the nomenclature of [14–16], namely noninteger J/N. To find an approximation for J/N, take

$$\Psi \approx \psi_{cr}\Theta(R_{\rm sol}-r)\prod_{j=1}^{n_V} e^{il_j\theta_j} \tag{12}$$

so the integral of Eq. (3) can be computed explicitly. With this ansatz, where $\Theta(\cdot)$ is the Heaviside step-function, the contribution from the different vortices is additive: $J = \psi_{cr}^2\sum_{j=1}^{n_V} l_j I_j$ with

$$I_j = \int_{r<R_{\rm sol}} \left(\frac{x(x-x_j)+y(y-y_j)}{(x-x_j)^2+(y-y_j)^2}\right) dxdy = \pi\left(R_{\rm sol}^2 - R_j^2\right), \tag{13}$$

where $R_j = \sqrt{x_j^2+y_j^2}$ and we have assumed $R_j < R_{\rm sol}$ (for $R_j > R_{\rm sol}$ the integral vanishes and therefore image vortices do not affect J in this approximation). Using $N \approx \pi R_{\rm sol}^2\psi_{cr}^2$

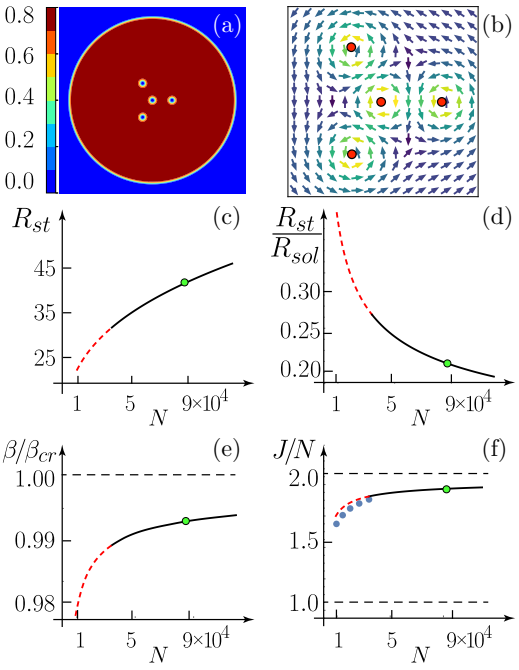

FIG. 2. A stationary and stable multivortex soliton, with $R_{\rm sol} = 192$, $R_{st} = 38$. Panel a) represents $|\Psi(x,y)|^2$ and panel b) is a quiver plot for the momentum, where we have enlarged the area around the vortices. (c)–(f) show how R_{st}, $R_{st}/R_{\rm sol}$, β and J/N change along the family. The dashed line indicates the unstable region, whereas the solid line is the stable region and the green dot marks the solution of (a) and (b). In (f), the horizontal line corresponds to the integer values $J/N = 2$, and the dotted line represents the approximation for J/N given in Eq. (14). We only draw the dotted line for small values of N since then it becomes hardly distinguishable from the solid line, to which it tends asymptotically.

and taking the $n = 3$, $l = -l_C = 1$ case, we find:

$$\frac{J}{N} \approx 2 - 3\frac{R_{st}^2}{R_{\rm sol}^2} \tag{14}$$

which, indeed, matches very well the numerical findings especially for large N, see Fig. 2, panel (e).

V. STABILITY

We have studied the stability of the stationary solutions by simulating long propagations, where long is defined by comparing with the period of rotation of the triangle without central antivortex. For small values of N, the vortex cores are too close to each other and the interaction between them ends up destabilizing the stationary solution. Within the unstable solutions, there are two qualitatively distinct behaviors. In both cases, the instability starts with an oscillation of the central antivortex around the central position. Then, for small enough N, the antivortex eventually pairs with one of the vortices and the pair gets a velocity large enough to escape, completely unravelling the initial configuration, as depicted in Fig. 3.

On the other hand, for an intermediate range of N, after oscillating for a while, the central antivortex, amazingly, returns to the center, reconstructing the initial configuration, albeit rotated. This produces a series of cycles of destabilization

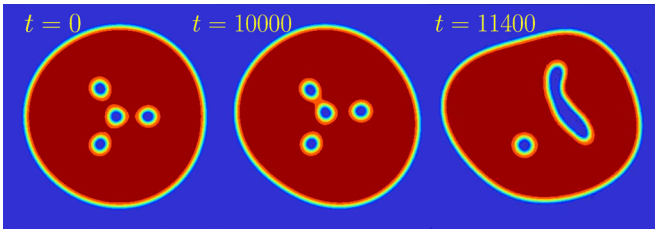

FIG. 3. Evolution of a stationary but unstable multivortex solution ($R_{\rm sol} = 64$, $R_{st} = 22.5$). See Ref. [46] for a video of the process.

and self-reconstruction such that the triangle remains static, then rotates, remains static again, etc. These cycles are nonlinear recurrences somehow reminiscent of those described in Refs. [53,54] in different setups. They are a two-dimensional generalization of a kind of phenomenon beautifully addressed in [55] in a one-dimensional setting: close to the transition of linear stability a linear eigenvalue becomes small and time-periodic orbits consisting of cycles of departure and reconstruction can appear. See Fig. 4 and Ref. [46] for illustration.

For larger values of N, our numerical simulations suggest that solutions are stable. In the Supplemental Material [46], we provide a video which shows how the profile depicted in Fig. 2 remains static and stable. In a second video, we use an analytic initial condition, Eq. (7) and check that the configuration is stable even if the initial condition is not exactly an eigenstate. Comparing both videos is interesting to visualize how good an approximation given by Eq. (7) can be.

It is worth mentioning that these are long propagation times, which amount to approximately a hundred full turns of the triangle if the central antivortex were absent. We have also checked stability with respect to dynamical processes. In Fig. 5, we simulate an example of collision of two stable multivortex solitons and show that their structure remains unchanged despite the resulting shakeup. Together, these computations provide strong evidence of the stability of the solutions.

VI. A NECESSARY CONDITION FOR THE EXISTENCE OF STATIC CONFIGURATIONS WITHIN A FLAT-TOP BACKGROUND

Up to now, we have studied the case of three vortices surrounding an antivortex in a cubic-quintic background. In

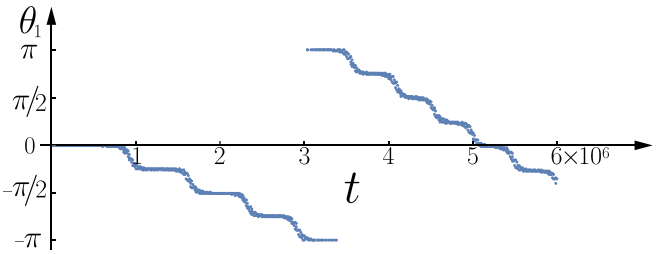

FIG. 4. Evolution in time of the polar angle at which one of the vertices of the equilateral triangle is located, for a stationary solution in the intermediate N region ($R_{\rm sol} = 96$, $R_{st} = 22.5$). As a qualitative description, the triangle remains initially in a static state, then undergoes rotation, comes to a halt, resumes rotation, and repeats this sequence cyclically.

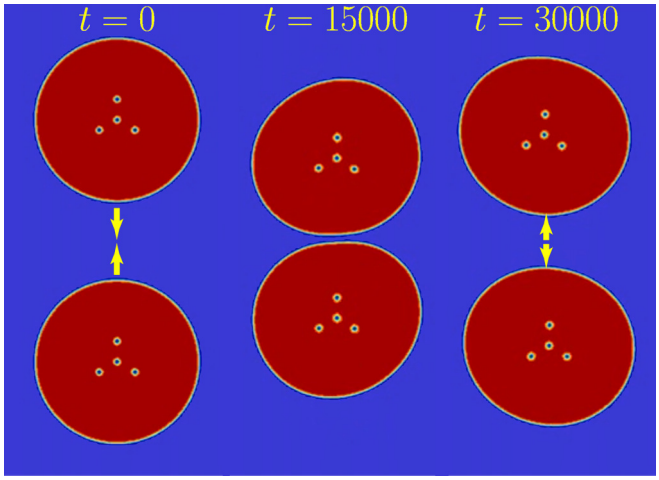

FIG. 5. Collision of two equal stable solitons ($R_{\rm sol} = 134$, $R_{st} = 34$) in phase opposition [46]. Initial velocities are $|v| = 0.005$. Collisions with different relative phases or larger velocities can result in droplet merging and the consequent unraveling of the vortex structures.

the limit $\beta \to \beta_{cr}$, both $R_{\rm sol}$ and R_{st} grow, the profile becomes increasingly flat-top, the soliton becomes larger and the interplay between the vortices and the boundary becomes negligible. In the limit $R_{\rm sol} \to \infty$ we can show that there is a necessary condition for the existence of stationary multivortex solutions to Eq. (10) or any other NLSE of the sort that admits flat-top solutions. The condition is very simple and relates the topological charges of all the phase dislocations in the configuration:

$$\left(\sum_{i=1}^{n_V} l_i\right)^2 = \sum_{i=1}^{n_V} l_i^2. \tag{15}$$

Notice that this condition is trivially satisfied by $n_V = 1$ (a vortex soliton). If $n_V > 1$, presence of both vortices and antivortices is required. If a stationary self-trapped solution can be continuosly connected to the limit with an infinitely large flat background, then Eq. (15) must be satisfied.

We now outline the proof of Eq. (15), which relies on a Pohozaev identity [56]. We use a result given in Ref. [57] for an NLSE of the form $-\beta\Psi = -\nabla^2\Psi + g(|\Psi|)\Psi$ when the asymptotic value of the wave function is $\lim_{r\to\infty} \Psi \approx \psi_{cr} e^{il\theta}$. A simple generalization of the result in Ref. [57] can be written as

$$\int_{\mathbb{R}_2} F dxdy = -\frac{\pi}{2} l^2 \psi_{cr}^2, \tag{16}$$

where $F(|\Psi|)$ is a function such that $\frac{dF(|\Psi|)}{d|\Psi|} = f(|\Psi|)$ and $F(\psi_{cr}) = 0$, with $f(|\Psi|) = -(\beta + g(|\Psi|))|\Psi|$. Let us apply this for vortices within a constant background, with the intervortex separation much larger than the size of the vortex core. Far from the vortex cores, $|\Psi| \approx \psi_{cr}$, and the contribution to the integral $\int F dxdy$ is negligible. Therefore, the integral can be written as a sum of the integrals around each vortex core: $\int_{\mathbb{R}_2} F dxdy = \sum_{i=1}^{n_V} \int_{S_i} F dxdy = -\frac{\pi}{2}\psi_{cr}^2 \sum_{i=1}^{n_V} l_i^2$, where S_i is a surface around each vortex which is far from the other vortices but much larger than the vortex cores. On the other hand,

applying the Pohozaev identity for the whole $x-y$ plane we get $\int_{\mathbb{R}_2} F dxdy = -\frac{\pi}{2}\psi_{cr}^2(\sum_{i=1}^{nv} l_i)^2$. Comparing both expressions, we immediately find the relation (15).

Please note that we utilized Eq. (16), which strictly holds only in the limit as $R_{\rm sol} \to \infty$, corresponding to vortices embedded in an infinite background. Nevertheless, when $R_{\rm sol}$ is significantly larger than the intervortex separation but finite, a similar approach can be employed by truncating the integral at a radius within the soliton but far from the vortices. Under these conditions, Eq. (16) serves as a reliable approximation, and its accuracy improves with the growth of $R_{\rm sol}$. If a stationary solution belongs to a family dependent on $R_{\rm sol}$, it can be continuously linked to a case with $R_{\rm sol} \to \infty$. Consequently, the Diophantine relation (15), which remains unaltered in a continuous deformation, must hold for the entire family.

Finally, it is worth noting that in the case of a single polygon and a central vortex, Eq. (15) is equivalent to Eq. (11). However, Eq. (15) becomes particularly useful in more complex configurations. For instance, consider a configuration of three nested triangles, two of them with $l = 1$ vortices at their vertices, and one with $l = -1$ antivortices. This configuration is known to exhibit a static solution for point vortices [25], and the topological charges appropriately satisfy (15). The investigation of the existence of self-trapped crystals with a similar arrangement of vortices is deferred to future work.

VII. CONCLUSION AND OUTLOOK

We have presented a one-parameter family of stationary solutions to the CQNLSE with four phase dislocations: three vortices and one antivortex (or viceversa). We have shown that there is a transition from instability to stability, with a peculiar intermediate region with nonlinear recurrences. We have also provided a simple but rather accurate expression for the angular momentum of these solitons, Eq. (14), and we have found a simple relation between the topological charges that is necessary for the existence of families of solutions of this sort, Eq. (15). These findings can pave the way for the search of more quiescent or spiraling multivortex solitons in the form of self-trapped vortex crystals, both in the CQNLSE or, more generally, for the NLSE with different nonlinear potentials. They can be applicable in different physical contexts, e.g., quantum droplets [58] where flat-top vortices also exist [59].

ACKNOWLEDGMENTS

We thank J. R. Salgueiro for collaboration at early stages of this work. This publication is part of the R&D&i project PID2020-118613GB-I00, funded by MCIN/AEI/10.13039/501100011033/. This work was also supported by Grant ED431B 2021/22 (Xunta de Galicia).

[1] B. A. Malomed, Low Temp. Phys. **48**, 856 (2022).
[2] N. J. Zabusky and M. D. Kruskal, Phys. Rev. Lett. **15**, 240 (1965).
[3] B. A. Malomed, Eur. Phys. J. Spec. Top. **225**, 2507 (2016).
[4] Y. V. Kartashov, G. E. Astrakharchik, B. A. Malomed, and L. Torner, Nat. Rev. Phys. **1**, 185 (2019).
[5] D. Mihalache, Rom. Rep. Phys. **73**, 403 (2021).
[6] J. F. Nye and M. V. Berry, Proc. Math. Phys. Eng. Sci. **336**, 165 (1974).
[7] Y. S. Kivshar and B. Luther-Davies, Phys. Rep. **298**, 81 (1998).
[8] G. A. Swartzlander Jr. and C. T. Law, Phys. Rev. Lett. **69**, 2503 (1992).
[9] V. Tikhonenko, J. Christou, B. Luther-Davies, and Y. S. Kivshar, Opt. Lett. **21**, 1129 (1996).
[10] M. R. Matthews, B. P. Anderson, P.C. Haljan, D.S. Hall, C.E. Wieman, and E. A. Cornell, Phys. Rev. Lett. **83**, 2498 (1999).
[11] B.P. Anderson, P.C. Haljan, C.A. Regal, D.L. Feder, L.A. Collins, C. W. Clark, and E. A. Cornell, Phys. Rev. Lett. **86**, 2926 (2001).
[12] A. S. Desyatnikov, Y. S. Kivshar, and L. Torner, in *Progress in Optics*, edited by E. Wolf (Elsevier, 2005), Chap. 5, Vol. 47, pp. 291–391.
[13] B. A. Malomed, Physica D **399**, 108 (2019).
[14] M. Soljačić and M. Segev, Phys. Rev. Lett. **86**, 420 (2001).
[15] L. Dong, D. Liu, W. Qi, L. Wang, H. Zhou, P. Peng, and C. Huang, Commun. Nonlinear Sci. Numer. Simul. **99**, 105840 (2021).
[16] L. Dong, Z. Du, and Z. Ren, Chaos Solit. Fractals **176**, 114184 (2023).
[17] D. Leykam and A. S. Desyatnikov, Opt. Lett. **36**, 4806 (2011).
[18] T. J. Alexander, A. S. Desyatnikov, and Y. S. Kivshar, Opt. Lett. **32**, 1293 (2007).
[19] B. Terhalle, T. Richter, A. S. Desyatnikov, D. N. Neshev, W. Krolikowski, F. Kaiser, C. Denz, and Y. S. Kivshar, Phys. Rev. Lett. **101**, 013903 (2008).
[20] D. Buccoliero, A. S. Desyatnikov, W. Krolikowski, and Y. S. Kivshar, Opt. Lett. **33**, 198 (2008).
[21] Y. V. Kartashov, B. A. Malomed, V. A. Vysloukh, M. R. Belić, and L. Torner, Opt. Lett. **42**, 446 (2017).
[22] J. R. Abo-Shaeer, C. Raman, J. M. Vogels, and W. Ketterle, Science **292**, 476 (2001).
[23] J. Scheuer and M. Orenstein, Science **285**, 230 (1999).
[24] L. Campbell and R. Ziff, Tech. Rep. No. LA-7384-MS, Los Alamos National Laboratory (LANL), Los Alamos, NM (United States) (1978).
[25] H. Aref, P. K. Newton, M. A. Stremler, T. Tokieda, and D. L. Vainchtein, Adv. Appl. Mech. **39**, 1 (2003).
[26] T. H. Havelock, Lond. Edinb. Dublin Philos. Mag. J. Sci. **11**, 617 (1931).
[27] E. Artemova and A. Kilin, Phys. Fluids **33**, 127105 (2021).
[28] H. Aref and M. van Buren, Phys. Fluids **17**, 057104 (2005).
[29] M. Quiroga-Teixeiro and H. Michinel, J. Opt. Soc. Am. B **14**, 2004 (1997).
[30] B. A. Malomed, D. Mihalache, F. Wise, and L. Torner, J. Opt. B **7**, R53 (2005).
[31] Pego and Warchall, J. Nonlinear Sci. **12**, 347 (2002).
[32] H. Michinel, J. R. Salgueiro, and M. J. Paz-Alonso, Phys. Rev. E **70**, 066605 (2004).
[33] T. Davydova and A. Yakimenko, J. Opt. A **6**, S197 (2004).
[34] E. L. Falcao-Filho, C. B. de Araújo, G. Boudebs, H. Leblond, and V. Skarka, Phys. Rev. Lett. **110**, 013901 (2013).

[35] A. S. Reyna and C. B. de Araújo, Adv. Opt. Phot. **9**, 720 (2017).
[36] H. Michinel, M. J. Paz-Alonso, and V. M. Pérez-García, Phys. Rev. Lett. **96**, 023903 (2006).
[37] Z. Wu, Y. Zhang, C. Yuan, F. Wen, H. Zheng, Y. Zhang, and M. Xiao, Phys. Rev. A **88**, 063828 (2013).
[38] A. Bulgac, Phys. Rev. Lett. **89**, 050402 (2002).
[39] R. Carretero-González, D. Frantzeskakis, and P. Kevrekidis, Nonlinearity **21**, R139 (2008).
[40] C. Josserand and S. Rica, Phys. Rev. Lett. **78**, 1215 (1997).
[41] H. Michinel, J. Campo-Táboas, R. García-Fernández, J.R. Salgueiro, and M.L. Quiroga-Teixeiro, Phys. Rev. E **65**, 066604 (2002).
[42] D. Novoa, H. Michinel, and D. Tommasini, Phys. Rev. Lett. **103**, 023903 (2009).
[43] V. Prytula, V. Vekslerchik, and V. M. Perez-Garcia, Phys. Rev. E **78**, 027601 (2008).
[44] N. G. Berloff, J. Phys. A **37**, 1617 (2004).
[45] A. Paredes, J. R. Salgueiro, and H. Michinel, Phys. Rev. E **107**, 044215 (2023).
[46] See Supplemental Material at http://link.aps.org/supplemental/10.1103/PhysRevE.109.024216 for videos showing the results of numerical simulations of evolution of Eq. (1) with different initial conditions, including those of Figs. 2–5.
[47] J. A. Fleck, J. Morris, and M. Feit, Appl. Phys. **10**, 129 (1976).
[48] E. Figueiras, D. Olivieri, A. Paredes, and H. Michinel, Eur. J. Phys. **39**, 055802 (2018).
[49] D. Neshev, A. Dreischuh, M. Assa, and S. Dinev, Opt. Commun. **151**, 413 (1998).
[50] A. J. Groszek, D. M. Paganin, K. Helmerson, and T. P. Simula, Phys. Rev. A **97**, 023617 (2018).
[51] W. Bao and Q. Du, SIAM J. Sci. Comput. **25**, 1674 (2004).
[52] L. Lehtovaara, J. Toivanen, and J. Eloranta, J. Comput. Phys. **221**, 148 (2007).
[53] A. Paredes, J. Blanco-Labrador, D. N. Olivieri, J. R. Salgueiro, and H. Michinel, Phys. Rev. E **99**, 062211 (2019).
[54] A. Biasi, O. Evnin, and B. A. Malomed, Phys. Rev. E **104**, 034210 (2021).
[55] D. E. Pelinovsky, V. V. Afanasjev, and Y. S. Kivshar, Phys. Rev. E **53**, 1940 (1996).
[56] S. I. Pokhozhaev, Dokl. Akad. Nauk. **165**, 36 (1965).
[57] A. Paredes, J. R. Salgueiro, and H. Michinel, Physica D **437**, 133340 (2022).
[58] Z.-H. Luo, W. Pang, B. Liu, Y.-Y. Li, and B. A. Malomed, Front. Phys. **16**, 32201 (2021).
[59] Y. Li, Z. Chen, Z. Luo, C. Huang, H. Tan, W. Pang, and B. A. Malomed, Phys. Rev. A **98**, 063602 (2018).